Journal of Biomedical Optics 7(1), 45–50 (January 2002)

Noninvasive total hemoglobin measurement

Kye Jin Jeon
Su-Jin Kim
Kun Kook Park
Samsung Advanced Institute of Technology
Medical Application Team
P. O. Box 111
Suwon 440-600, Korea

Jong-Won Kim
Samsung Medical Center
Department of Clinical Pathology
Seoul 135-230, Korea

Gilwon Yoon
Samsung Advanced Institute of Technology
Medical Application Team
P. O. Box 111
Suwon 440-600, Korea

Abstract. Wavelength selection and prediction algorithm for determining total hemoglobin concentration are investigated. A model based on the difference in optical density induced by the pulsation of the heart beat is developed by taking an approximation of Twersky's theory on the assumption that the variation of blood vessel size is small during arterial pulsing. A device is constructed with a five-wavelength light emitting diode array as the light source. The selected wavelengths are two isobestic points and three in compensation for tissue scattering. Data are collected from 129 outpatients who are randomly grouped as calibration and prediction sets. The ratio of the variations of optical density between systole and diastole at two different wavelengths is used as a variable. We selected several such variables that show high reproducibility among all variables. Multiple linear regression analysis is made in order to predict total hemoglobin concentration. The correlation coefficient is 0.804 and the standard deviation is 0.864 g/dL for the calibration set. The relative percent error and standard deviation of the prediction set are 8.5% and 1.142 g/dL, respectively. We successfully demonstrate the possibility of noninvasive hemoglobin measurement, particularly, using the wavelengths below 1000 nm.
[DOI: 10.1117/1.1427047]

Keywords: noninvasive; hemoglobin; isobestic point; pulsation; Twersky's theory.

Paper JBO-102106 received Apr. 18, 2001; revised manuscript received Aug. 7, 2001; accepted for publication Aug. 24, 2001.

1 Introduction

Measurement of the hemoglobin concentration is important since it provides information on the total oxygen-carrying ability and anemia. Total hemoglobin is used as a parameter to screen people who donate blood and are routinely being monitored during the treatment of patients with hemorrhaging or vascular and orthopedic surgery where a large amount of blood loss can occur. In the clinical laboratory, the hemoglobin concentration is usually measured by the hemoglobin cyanide (HiCN) method.[1] Hemoglobin must be monitored during transfusion. Therefore, it is desirable to measure hemoglobin continuously. Noninvasive measurement may be needed for the patients in the ERs, ICUs and of the postoperative follow-up.

There are some commercialized whole-blood hemometers by using blood taken from the finger.[2] However, there have been only a few investigations regarding noninvasive hemoglobin measurement. Near-infrared diffuse reflectance spectra measured on the patient forearm at 575–1100 nm were analyzed using partial least squares regression.[3] A single patient calibration model was acceptable, but the multisubject model produced a large prediction error. Hemoglobin is a dominant absorber in blood showing high absorptivity at 575–1100 nm. It is expected that the absorption spectra varies at what time frame of arterial pulse cycle the measurement is taken. In our study, hemoglobin is measured noninvasively using an arterial pulse signal considering light scattering from the red blood cells (RBCs). According to Beer's law, the ratio of two absorbances at the isobestic wavelengths is given as a constant with no relation to the hemoglobin concentration. As RBCs are the center of scattering and absorption,[4–6] the ratio is not a constant but depends on the density of RBCs. By approximating Twersky's theory, we develop a method of predicting the total hemoglobin concentration based on the arterial pulse measurement.

2 Theory

The optical density of whole blood is 7–25 times larger than the hemoglobin solution for the same pathlength and hemoglobin concentration.[7] This is explained by the light scattering of RBCs at 600–1000 nm. Multiple scattering by large, low-refracting, and absorbing particles is well explained by Twersky's theory that is based on the electromagnetic wave theory.[8–10]

Our proposed theory is based on Twersky's theory whose approximation is derived on the assumption that the variation of the arterial diameter generated between the systolic and diastolic periods is small. First, a finger and arterial model is introduced and an expression in terms of the hemoglobin concentration is developed. When incoherent light is irradiated on a finger, light is highly diffused through tissue and bone. Light intensity is modulated by the variation of the thickness of the arterial vessel according to the heartbeat.

2.1 Finger Model

Detected light is classified into two groups according to the path of light; photons travel through the arterial vessel and are

Address all correspondence to Gilwon Yoon. Tel: 82-31-280-6520; Fax: 82-31-280-9208; E-mail gyoon@sait.samsung.co.kr

1083-3668/2002/$15.00 © 2002 SPIE

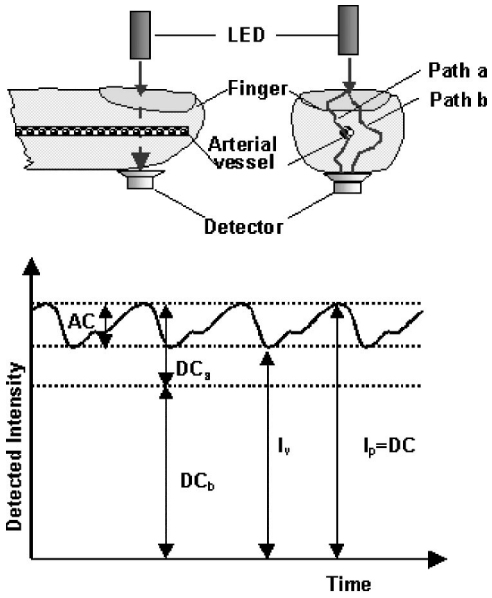

Fig. 1 Finger model.

modulated by the arterial pulse (''path a'' in Figure 1), photons do not pass the arterial vessel (''path b'' in Figure 1). The direct current (DC) level of path a (DC_a) and the DC level of path b (DC_b) can be expressed as follows:

$$DC_a = f(r_a, r_f, \lambda)DC, \quad DC = DC_a + DC_b, \tag{1}$$

where r_a is the radius of the arterial blood vessel, r_f is the radius of the finger, $f(r_a, r_f, \lambda)$ is the portion of light that travels through an arteriole vessel and is related to the geometry of the finger and wavelength, and DC is the total transmitted DC level. The ratio of AC (alternating current) to DC_a represents the difference in the total optical density between systole and diastole. The variation of total optical density is given by

$$\Delta OD_{tot} = AC/DC_a = [1/f(r_a, R_f, \lambda)]AC/DC \equiv (1/f)R, \tag{2}$$

where, R is defined as the ratio of AC and DC.

Real time monitoring of the variation of the arterial blood vessel thickness and the individuality compensation of the finger is very difficult. In this study, we are using the ratio between AC and DC components as a parameter as used in the pulse oximeter case.[11]

$$R_{ij} \equiv \frac{R_i}{R_j} = \frac{AC_i/DC_i}{AC_j/DC_j} = \frac{f(r_a, r_f, \lambda_i)\Delta OD_{tot,i}}{f(r_a, r_f, \lambda_j)\Delta QD_{tot,j}} \approx \frac{\Delta OD_{tot,i}}{\Delta OD_{tot,j}}, \tag{3}$$

where $f(r_a, r_f, \lambda_i) \approx f(r_a, r_f, \lambda_j)$ is assumed. The alternating part is generated due to the pulsatile portion of blood. The optical pathlength varies depending on the wavelength, finger shape, color, composition, etc. However, it is expected that such variations will influence both AC and DC to the same degree. When AC/DC is used as a parameter, such influences will be minimized. Difference induced by the variation of arterial blood vessel thickness becomes negligible when we use the ratio of ΔOD_{tot}'s at two different wavelengths.

2.2 Arterial Model

When light transports through whole blood, it experiences multiple scattering and absorption. Light scattering takes place by the mismatch of the refractive indices between blood plasma and RBCs. When the collimated light enters whole blood whose path length is D, total attenuation of the incident light ($OD_{tot\ atte}$) can be expressed according to Twersky's theory

$$OD_{tot\ atte} = \log(I_0/I_c) = \varepsilon CD + aDH(1-H), \tag{4}$$

where I_c, I_0: transmitted and incident collimated light intensity, respectively, ε: extinction coefficient, C: concentration of absorbing blood component, a: constant dependent upon particle size, refracting indices of particle (n_{Hb}), suspending medium (n_{plasma}), and wavelength (λ). According to Twersky's formulation, $a = (4\pi 2L/\lambda^2)(n'-1)^2$ and $n' = n_{Hb}/n_{plasma}$, L is a shape factor of RBCs, H: fractional hematocrit and for RBCs where the hemoglobin concentration (g/dL) is 35 H.

In Eq. (4), the first term is Beer's law expression for absorption by hemoglobin and the second term describes the attenuation of collimated light due to scattering.

When the detector receives scattered light within a certain solid angle, Eq. (4) becomes more complex since backscattering has to be considered[12] and is given by the following equation

$$OD_{tot} = \log(I_0/I) = \varepsilon CD - \log[(1-q)10^{-aDH(1-H)} + q10^{-2q'\varepsilon CDaDH(1-H)/(2\varepsilon CD + aDH(1-H))}], \tag{5}$$

where q is a constant dependent upon the particle size, n_{Hb}, n_{plasma}, λ, and the photodetector aperture angle and q' are a parameter of the particular design with its value between 0 and 1. q' couples absorbance and scattering and it depends primary on λ and the spectral properties of the light source. In Figure 2, optical density due to scattering (OD_{sct}) is calculated from Eq. (5) for a different variation of the arterial vessel thickness using the values of the optical parameters given by Steinke et al.[12] at 660, 805, 880, and 940 nm. As the thickness becomes smaller, the curve shape approaches to a parabola as illustrated in Figure 2 which is given as the following approximation:

$$OD_{tot} = \log(I_0/I) = \varepsilon D + kaDH(1-H), \tag{6}$$

where k is related to the optical design, sample thickness, scattering properties, and wavelength. Values of k are obtained by the fitting curves shown in Figure 2 and are summarized in Table 1. Figure 3 shows k in terms of the sample thickness in respect to the wavelength. k values are different at a large thickness, but approach the same value as the thickness becomes smaller.

It is known that the diameter of an artery in a finger or toe is approximately 0.3–1.5 mm and the diameter variation is several percent during heartbeat.[13] So we can apply expression (6) for the variation of the optical density between systolic and diastolic periods because the diameter variation regarding the heartbeat is expected to be smaller than 0.5 mm. This hypothesis is applied and the difference in optical densities between the systolic and diastolic periods is derived in terms of the transmitted intensity

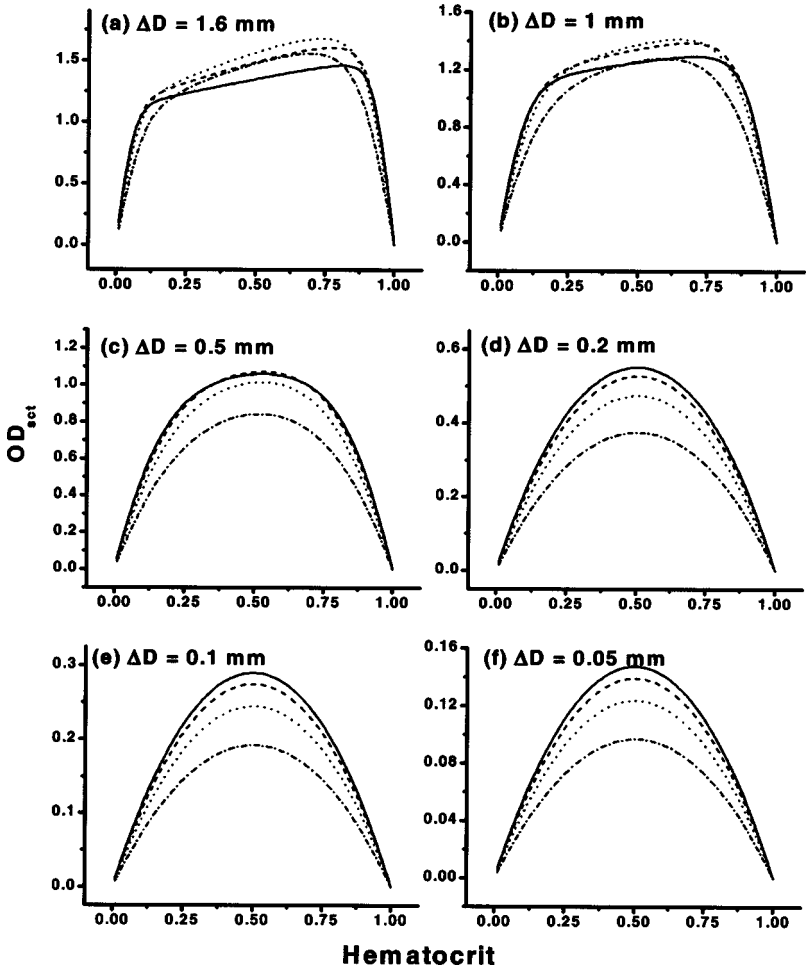

Fig. 2 Optical density due to scattering (OD_{sct}) with various thickness of the blood sample using the value of optical parameter acquired by J. M. Steinke at wavelength 660, 805, 880, and 940 nm [(solid line) 660 nm, (dashed line) 805 nm, (dotted line) 880 nm, (dash-dotted line) 940 nm].

$$I_\nu = I_p 10^{-\Delta \mathrm{OD}_{\mathrm{tot}}}, \quad \Delta \mathrm{OD}_{\mathrm{tot}} \approx (1/\ln 10)\left(\frac{I_p - I_\nu}{I_\nu}\right), \qquad (7)$$

where I_p is the transmitted intensity at the diastolic state and I_ν is that at the systolic state.

Table 1 Calculated *k* value of each curve fitted with Figure 2 to the parabolic function is shown with respect to the sample thickness.

	Wavelength (nm)			
Sample thickness (mm)	660	805	880	940
0.5	0.611 61	0.673 32	0.729 77	0.774 85
0.2	0.842 37	0.864 12	0.877 06	0.878 84
0.1	0.890 88	0.903 17	0.908	0.902 68
0.05	0.9094	0.918 32	0.920 43	0.912 78
0.01	0.921 88	0.928 67	0.929 13	0.920 14
0.001	0.9242	0.930 41	0.930 53	0.922 03

The ratio between the two wavelengths λ_i and λ_j is given in Eq. (3), $\mathrm{AC}_i = I_{p,\lambda i} - I_{\nu,\lambda i}$, and $\mathrm{DC}_i = I_{\nu,\lambda i}$:

$$R_{ij} = \frac{R_i}{R_j} = \frac{\mathrm{AC}_i/\mathrm{DC}_i}{\mathrm{AC}_j/\mathrm{DC}_j} \approx \frac{\Delta \mathrm{OD}_{\mathrm{tot},\lambda i}}{\Delta \mathrm{OD}_{\mathrm{tot},\lambda j}}. \qquad (8)$$

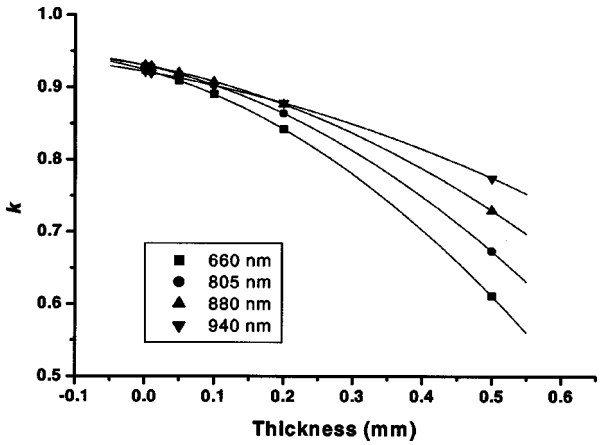

Fig. 3 *k* value of each curve fitted with Figure 2 to a parabolic function is demonstrated as the varying sample thickness.

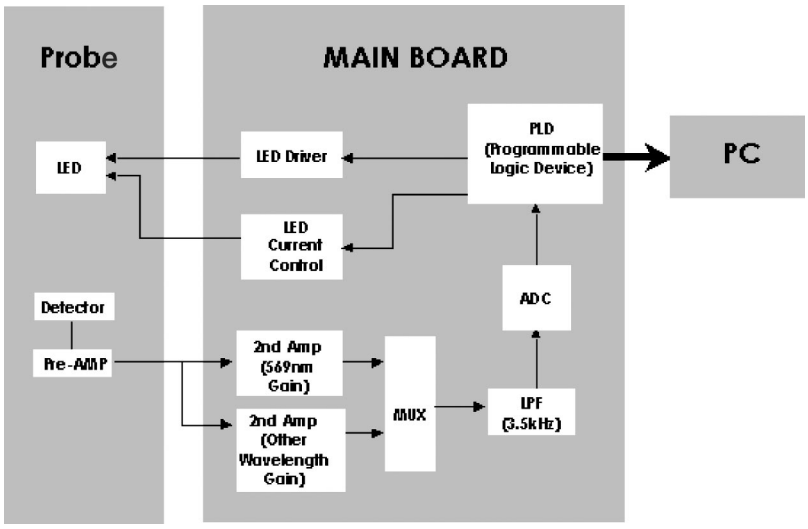

Fig. 4 Noninvasive hemoglobin measurement system.

In case of 569 and 805 nm, Eq. (9) can be denoted by

$$R_{569.805}=\frac{\mathrm{AC}_{569}/\mathrm{DC}_{569}}{\mathrm{AC}_{805}/\mathrm{DC}_{805}} \approx \frac{\varepsilon_{569}C\Delta D+k_{569}a_{569}\Delta DH(1-H)}{\varepsilon_{805}C\Delta D+k_{805}a_{569}\Delta DH(1-H)} = \frac{35\varepsilon_{569}+k_{569}a_{569}(1-H)}{35\varepsilon_{805}+k_{805}a_{805}(1-H)}, \quad (9)$$

where ΔD is the thickness variation of the arterial vessel between the systolic and diastolic periods. k depends on the optical design of the system and a is the RBCs shape function. In the case of the finger, further information at more wavelengths to compensate for the tissue influence is required since the arterial vessel is embedded in the tissue.

3 Methods

A hardware prototype is developed based on the transmission measurement through a finger. The system consists of a finger probe and main board as seen in Figure 4. The probe houses a light source which is a custom-designed light emitting diode (LED) array (Epitex, Inc.) of 569, 660, 805, 940, and 975 nm. A detecting part is composed of a Si photodiode and preamplifier. Each LED turns on and off consecutively. The frequency, duration time and order of LEDs on and off are controlled by the software. The main board consists of the power control part and signal processing part and is designed to have an interface with a notebook computer (PC). The power control part supplies electrical power to the probe and drives the LED array. The signal processing part carries out the amplification of the detected signal and low pass filtering and A/D acquisition with a 16-bit resolution. A programmable logic device is introduced to control the main board and to control the interface with PC. The schematic of the system is shown in Figure 4.

The acquired data are averaged and the information for each wavelength is separated. The time variant noise that is induced from the respiration and minute finger movement are potential sources of error. Digital filtering and the algorithm of compensating for the base line drift are applied. The algorithm used for the compensation of the base line drift is a moving average filtering.

4 Result and Analysis

In vivo data were collected from 129 patients at Samsung Medical Center for 3 days. Five measurements were made per person with each measurement of 8 seconds. The reference value of the hemoglobin concentration is obtained from the hemoglobin cyanide method which is commonly used in the clinical laboratory. Measured data are divided into two groups, i.e., the calibration and prediction sets. 75% of the data including low and high hemoglobin concentration are randomly selected as the calibration set. The rest of the data are used as the prediction set.

Figure 5 shows the average value with the deviation of normalized R values for all the patients. The normalized R value is acquired by dividing each R_i ($=\mathrm{AC}_i/\mathrm{DC}_i$ where i is the wavelength index) with the sums of R's at four wave-

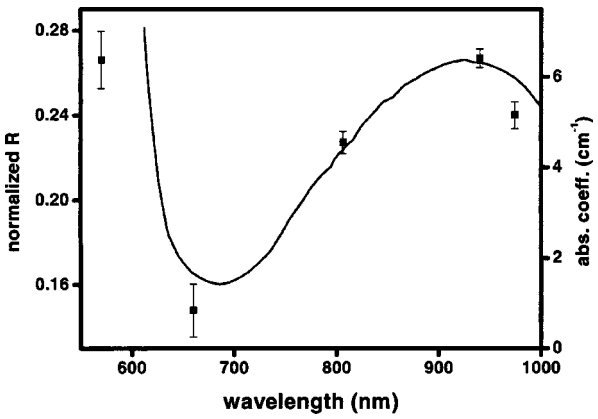

Fig. 5 Normalized R values of all patients (average value with the deviation). The solid line shows the absorption coefficient of oxygenated hemoglobin with a 15 g/dL concentration.

Table 2 The best subset of the regression with all five variables, where R^2 is the square of correlation coefficient R. R^2-adj is a modified R^2 that has been adjusted for the number of predictors in the model. $C-p$ is expressed as the summation of mean-squared errors of fitted response divided by the variance of the error term. SD is the error standard deviation.

No.	Var	R^2	R^2-adj	$C-p$	SD	R_{12}	R_{13}	R_{14}	R_{15}	R_{34}
1	1	31.1	30.9	376.9	1.2019	x				
2	1	26.1	25.9	433.0	1.2446					x
3	2	45.9	45.7	211.3	1.0659				x	x
4	2	44.3	44.1	229.2	1.0815			x	x	
5	3	64.5	64.2	4.1	0.86527		x	x	x	
6	3	64.3	64.0	5.9	0.86716			x	x	x
7	4	64.6	64.3	4.3	0.86439	x	x	x	x	
8	4	64.5	64.2	5.4	0.86559		x	x	x	x
9	5	64.6	64.2	6.0	0.86513	x	x	x	x	x

lengths except 660 nm. For example, normalized $R_1 = R_1/(R_1+R_3+R_4+R_5)$. The wavelength index is 1 at 569 nm, 2 at 660 nm, 3 at 805 nm, 4 at 940 nm, and 5 at 975 nm. 660 nm is very sensitive to the oxygenated state of hemoglobin. We wanted to exclude this influence. When the absorption coefficient of 100% oxyhemoglobin at five wavelengths is compared with the normalized R value, the results show similar patterns except at 569 nm. At 569 nm unlike at other wavelengths, the normalized R-value graph is off from the pattern compared with the graph of the absorption of the oxygenated hemoglobin (see Figure 5). From Eqs. (1), (2), and (3), we can obtain the following:

$$R_1 = \frac{\mathrm{AC}_{\lambda_1}}{\mathrm{DC}_{a,\lambda_1}+\mathrm{DC}_{b,\lambda_1}} = \frac{\Delta \mathrm{OD}_{\mathrm{tot}\,\lambda_1}}{1+\mathrm{DC}_{b,\lambda_1}/\mathrm{DC}_{a,\lambda_1}} = f(r_a, r_b, \lambda_1)\Delta \mathrm{OD}_{\mathrm{tot}\lambda_1}. \quad (10)$$

DC_b (a proportion of detected light at 569 nm that does not travel through an arterial vessel) may be larger than DC_a (a proportion of detected light at 569 nm that experience an arterial vessel) and AC compared with those at other wavelengths. Therefore, it appears that measured normalized R_{569} is small because of small $f(r_a, r_h, \lambda_1)$ in Eq. (10) compared with other wavelengths. In Eq. (3), $f(r_a, r_f, \lambda)$ is not usually the same with respect to the wavelength, but depends on the wavelength and geometry. By this reason, two isobestic points of 569 nm(λ_1) and 805 nm(λ_3) are insufficient to predict the hemoglobin concentration *in vivo*. To compensate for the tissue-dependency, more wavelengths like 660 nm(λ_2), 940 nm(λ_4), and 975 nm(λ_5) are added where the light penetration is deep enough. The ratio of R, i.e., $R_{ij} \equiv R_i/R_j$ that is an indicator on the relative variations of the optical density between systole and diastole at two wavelengths is used as the variable. We selected five variables ($R_{12}, R_{13}, R_{14}, R_{15}$, and R_{34}) that show high reproducibility among all variables of ratio (R_{ij}). This process was done by repeated measure of ANOVA. Multiple linear regression analysis using MINITAB (Minitab Inc.) was made. For the calibration set, the best subsets of regression with five variables are listed in Table 2. The result with four variables shows the best regression with a correlation coefficient of 0.804 and the standard deviation of 0.864 g/dL. To predict the concentration of the prediction set, five calibration models are established. The result of the prediction is summarized in Table 3, the relative prediction error is $\pm 8.5\%$ with the standard deviation of ± 1.142 g/dL for the case of three variables that yields the best prediction. The prediction of hemoglobin is displayed in terms of the calibration and prediction sets and residuals (Figure 6 for three variables). Our investigation demonstrates that noninvasive monitoring of the hemoglobin concentration using discrete wavelengths is feasible. However, the accuracy needs to be improved since the clinically acceptable percent error of hemoglobin is $\pm 7\%$.[14] The regression analysis shows a tendency of overestimation at a low hemoglobin concentration and underestimation at a higher hemoglobin concentration. In this regard, further investigation will be followed.

Table 3 The result of the prediction set using five calibration models.

No. of variable	% error	SD	Variables
1	13.206 89	1.741 32	R_{12}
2	11.309 79	1.506 84	R_{15}, R_{34}
3	8.503 16	1.142	R_{13}, R_{14}, R_{15}
4	8.649 77	1.153 22	$R_{12}, R_{13}, R_{14}, R_{15}$
5	9.343 09	1.224 21	$R_{12}, R_{13}, R_{14}, R_{15}, R_{34}$

5 Summary

We investigate the calculation algorithm and wavelength selection for the determination of the total hemoglobin concentration noninvasively. For this purpose, a model based on the difference of the optical densities induced by the pulsation of a heartbeat is developed by taking an approximation of Twersky's theory on the assumption that the variation of the blood vessel thickness is small during the arterial pulsation. By using the ratio of the optical density variations between the systolic and diastolic periods at two different wavelengths, the influence of the individual finger structure can be compensated. Wavelengths under a 1000 nm region are chosen; two isobestic points of 569 and 805 nm, and 660, 940, and 975 nm in compensation of tissue scattering. Five variables (R_{ij}: the ratio of optical density variations at two wavelengths) having reproducibility are selected for calibration and prediction. A finger probe containing a LED array and compact control electronics are developed for experimental verification. The results with 129 persons are; the correlation coefficient is 0.804 and the standard deviation is 0.864 g/dL for the calibration set, and the standard deviation of the prediction set is 1.142 g/dL. We demonstrate the possibility of developing a noninvasive and compact device for monitoring the total hemoglobin, particularly, using the wavelength below 1000 nm

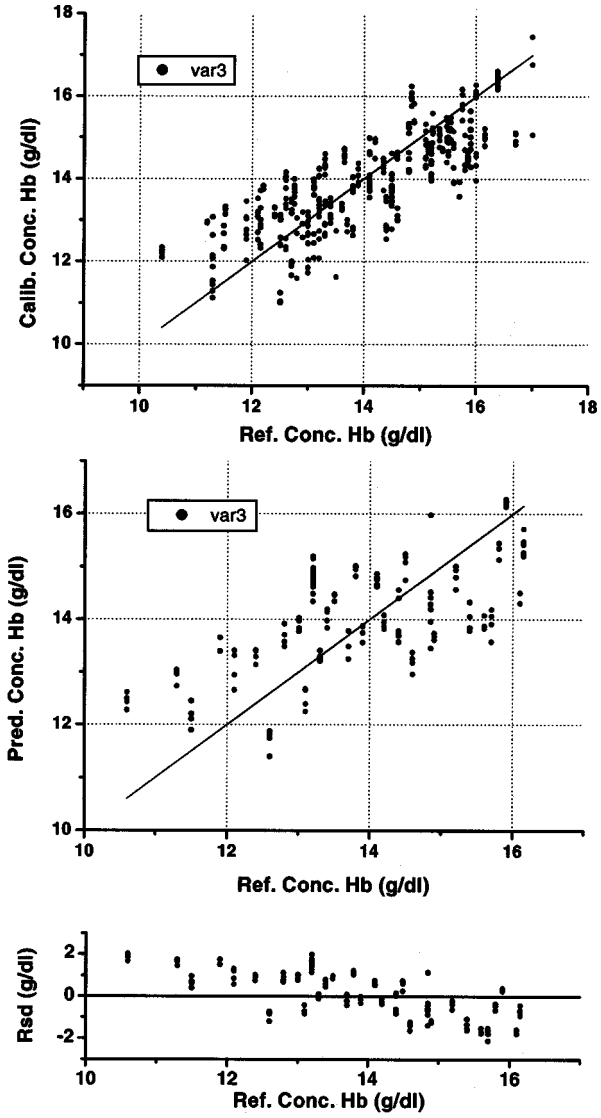

Fig. 6 Determination of total hemoglobin: Calibration set and prediction set and residual of the prediction with three variables.

with all optical means. Yet there are further investigations to be done for this study to be led as a commercially viable device. The calibration and prediction should be extended to include the subsets of the lower and higher hemoglobin concentration than the normal physiological range. The population size should be far more exceeding than the current investigation as well as diverse population.

Acknowledgments

This work is supported in part by National Research Laboratory Program of Ministry of Science and Technology, Korea.

References

1. E. J. van Kampen and W. G. Zijlstra, ''Spectrophotometry of hemoglobin and hemoglobin derivatives,'' in *Advances in Clinical Chemistry*, A. L. Latner and M. K. Schwartz, Eds., Vol. 23, pp. 200–219, Academic, New York (1983).
2. J. L. Schmalzel, J. M. Steinke, V. T. Randal, and A. P. Shepherd, ''An optical hemoglobinmeter for whole blood,'' *Am. J. Physiol.* **257**, H1306–H1311 (1989).
3. S. Zhang, B. R. Soller, S. Kaur, K. Perras, and T. J. Vander Salm, ''Investigation of noninvasive *in vivo* blood hematocrit measurement using NIR reflectance spectroscopy and partial least-squares regression,'' *Appl. Spectrosc.* **54**(2), 294–299 (2000).
4. A. Roggan, M. Friebel, K. Dorschel, A. Hahn, and G. Muller, ''Optical properties of circulating human blood in the wavelength range 400–2500 nm,'' *J. Biomed. Opt.* **4**(1), 36–46 (1999).
5. A. G. Borovoi, E. I. Naats, and U. G. Oppel, ''Scattering of light by red blood cell,'' *J. Biomed. Opt.* **3**(3), 364–372 (1998).
6. J. T. Kuenstner and K. H. Norris, ''Spectrophotometry of human hemoglobin in the near infrared region from 1000 to 2500 nm,'' *J. Near Infrared Spectrosc.* **2**, 59–65 (1994).
7. K. Kramer, J. O. Elam, G. A. Saxton, and W. N. Elam, Jr., ''Influence of oxygen saturation, erythrocyte concentration and optical depth upon the red and near-infrared light transmittance of whole blood,'' *Am. J. Physiol.* **165**, 229–246 (1951).
8. V. Twersky, ''Multiple scattering of waves and optical phenomena,'' *J. Opt. Soc. Am.* **52**, 145–170 (1962).
9. V. Twersky, ''Interface effects in multiple scattering by large, low-refracting, absorbing particle,'' *J. Opt. Soc. Am.* **60**, 908–914 (1970).
10. V. Twersky, ''Absorption and multiple scattering by biological suspensions,'' *J. Opt. Soc. Am.* **60**, 1084–1093 (1970).
11. O. Wieben, ''Light absorbance in pulse oximetry,'' in *Design of Pulse Oximeters*, J. G. Webster, Ed., Chap. 4, pp. 40–55, Institute of Physics Publishing, Bristol (1997).
12. J. M. Steinke and A. P. Shepherd, ''Role of light scattering in whole blood oximetry,'' *IEEE Trans. Biomed. Eng.* **BME-33**(3), 294–301 (1986).
13. Y. Tardy, J. J. Meister, F. Perret, H. R. Brunner, and M. Arditi, ''Noninvasive estimate of the mechanical properties of peripheral arteries from ultrasonic and photoplethysmographic measurements,'' *Clin. Phys. Physiol. Meas.* **12**, 39–54 (1991).
14. *Tietz textbook of clinical chemistry*, C. A. Burtis and E. R. Ashwood, Eds., Chap. 13, Saunders, Philadelphia (1999).